

## Initial Example of a Triangular Single-Molecule Magnet from Ligand-Induced Structural Distortion of a $[\text{Mn}^{\text{III}}_3\text{O}]^{7+}$ Complex

Theocharis C. Stamatatos,<sup>†</sup> Dolos Foguet-Albiol,<sup>‡</sup> Constantinos C. Stoumpos,<sup>†</sup>  
Catherine P. Raptopoulou,<sup>§</sup> Aris Terzis,<sup>§</sup> Wolfgang Wernsdorfer,<sup>#</sup> Spyros P. Perlepes,<sup>\*,†</sup> and  
George Christou<sup>\*,‡</sup>

Department of Chemistry, University of Patras, 26504 Patras, Greece, Department of Chemistry, University of Florida, Gainesville, Florida 32611-7200, Institute of Materials Science, NCSR "Demokritos", 15310 Aghia Paraskevi Attikis, Greece, and Laboratoire Louis Néel-CNRS, 38042 Grenoble, Cedex 9, France

Received August 24, 2005; E-mail: christou@chem.ufl.edu; perlepes@patreas.upatras.gr

Single-molecule magnets (SMMs) are individual molecules that function as nanoscale magnetic particles.<sup>1,2</sup> They derive their properties from the combination of a large ground-state spin ( $S$ ) and a magnetoanisotropy of the Ising-type (negative zero-field splitting parameter,  $D$ ).<sup>1</sup> They also display quantum tunneling of magnetization (QTM)<sup>3</sup> and quantum phase interference,<sup>4</sup> properties of the microscale. SMMs of various types and metal topologies are now known, with most being Mn species. There are, however, no triangular SMMs; numerous oxide-centered triangular  $[\text{M}_3\text{O}(\text{O}_2\text{-CR})_6\text{L}_3]^{n+}$  ( $n = 0, 1$ ) complexes are known for many transition metals,<sup>5a</sup> but antiferromagnetic exchange interactions within the  $[\text{M}_3\text{O}]$  core lead to small  $S$  values, and they are therefore not SMMs.<sup>5</sup> It is thus tempting to conclude that this common triangular  $[\text{M}_3\text{O}]$  structural topology can never lead to SMMs, but we show in the present work that relatively small, ligand-imposed structural distortions can alter the sign of the exchange interactions and "switch on" the SMM property.

We have been exploring the use of 2-pyridyl oximes<sup>6</sup> in the synthesis of 3d metal clusters, and we can now report that methyl 2-pyridyl ketone oxime (mpkoH) has yielded a new triangular  $[\text{Mn}^{\text{III}}_3\text{O}]$  product. This is very unusual in being ferromagnetically coupled with a resultant  $S = 6$  ground-state spin and is indeed the first triangular SMM.

The reaction of  $[\text{Mn}_3\text{O}(\text{O}_2\text{CMe})_6(\text{py})_3](\text{ClO}_4)$  (**1**) with mpkoH (3 equiv) in MeOH/MeCN (1:2 v/v) gave a dark-brown solution. This was evaporated to dryness under reduced pressure, and the residue was dissolved in  $\text{CH}_2\text{Cl}_2$  and layered with *n*-hexane. After 2 days, dark-brown crystals of  $[\text{Mn}_3\text{O}(\text{O}_2\text{CMe})_3(\text{mpko})_3](\text{ClO}_4) \cdot 3\text{CH}_2\text{Cl}_2$  (**2**· $3\text{CH}_2\text{Cl}_2$ ) were isolated in 80–90% yield. The structure<sup>7</sup> of **2**· $3\text{CH}_2\text{Cl}_2$  (Figure 1) consists of a near-equilateral  $\text{Mn}_3$  triangle capped by  $\mu_3\text{-O}^{2-}$  ion O61. Each edge is bridged by an  $\eta^1\text{:}\eta^1\text{:}\mu\text{-MeCO}_2^-$  group and an  $\eta^1\text{:}\eta^1\text{:}\eta^1\text{:}\mu\text{-mpko}^-$  group, whose pyridyl ring is bound terminally to a Mn. O61 is 0.295 Å above the  $\text{Mn}_3$  plane. The  $\text{Mn}^{\text{III}}$  oxidation states and  $\text{O}^{2-}$  protonation level were established by bond valence sum (BVS) calculations,<sup>8,9</sup> charge considerations, and the presence of  $\text{Mn}^{\text{III}}$  Jahn–Teller elongation axes (O1–Mn1–O31, O11–Mn2–O51, O21–Mn3–O42). The isostuctural propionate analogue was prepared in an identical manner.

Variable-temperature DC magnetic susceptibility data were collected on dried **2** in the temperature range of 5.0–300 K in an applied field of 1 kG (0.1 T).  $\chi_{\text{M}}T$  is 13.01  $\text{cm}^3 \text{mol}^{-1} \text{K}$  at 300 K, increasing on cooling to a maximum of 19.39  $\text{cm}^3 \text{mol}^{-1} \text{K}$  at 30.0 K, and then decreasing to 17.41  $\text{cm}^3 \text{mol}^{-1} \text{K}$  at 5.00 K.<sup>9</sup> This indicates ferromagnetic exchange interactions within **2** to give an  $S = 6$  ground state, which is consistent with the 30.0 K value (spin-

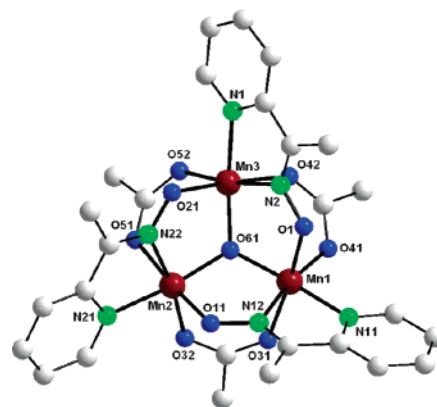


**Figure 1.** Molecular structure of **2**. Color code: brown, manganese; blue, oxygen; green, nitrogen; gray, carbon.

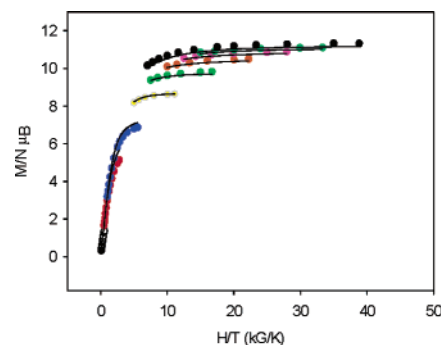


**Figure 2.** Plot of  $M/N\mu_{\text{B}}$  versus  $H/T$  for complex **2** at 7 (black dot), 6 (dark green dot), 5 (magenta dot), 4 (orange dot), 3 (light green dot), 2 (yellow dot), 1 (blue dot), 0.5 (red dot), and 0.1 (open dot) tesla. The solid lines are the fit of the data.

only ( $g = 2$ ) value for  $S = 6$  is 21  $\text{cm}^3 \text{mol}^{-1} \text{K}$ ). The low temperature decrease is assigned to Zeeman effects, zero-field splitting, and/or weak intermolecular interactions. The data were fit to the theoretical expression for a  $3\text{Mn}^{\text{III}}$  isosceles triangle.<sup>9,10</sup>

To confirm the ground state of **2**, magnetization ( $M$ ) data were collected in the 0.1–7 T and 1.8–10.0 K ranges, and these are plotted as  $M/N\mu_{\text{B}}$  versus  $H/T$  in Figure 2. The data were fit by matrix-diagonalization to a model that assumes only the ground state is populated, includes axial zero-field splitting ( $D\hat{S}_z^2$ ) and the Zeeman interaction, and carries out a full powder average; the spin Hamiltonian is given by eq 1, where  $\mu_{\text{B}}$  is the Bohr magneton and  $\mu_0$  is the vacuum permeability,  $\hat{S}_z$

$$H = D\hat{S}_z^2 + g\mu_{\text{B}}\mu_0\hat{S}_zH_z \quad (1)$$

is the easy-axis spin operator, and  $H_z$  is the applied field. The fit (solid lines in Figure 2) gave  $S = 6$ ,  $g = 1.92$ , and  $D = -0.34 \text{ cm}^{-1}$ .<sup>11</sup>

<sup>†</sup> University of Patras.

<sup>‡</sup> University of Florida.

<sup>§</sup> NCSR "Demokritos".

<sup>#</sup> Laboratoire Louis Néel-CNRS.

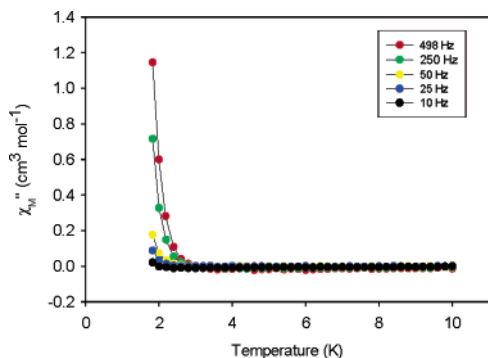


**Figure 3.** Plot of the out-of-phase ( $\chi_M''$ ) AC susceptibility signal versus temperature for a microcrystalline sample of complex **2**.

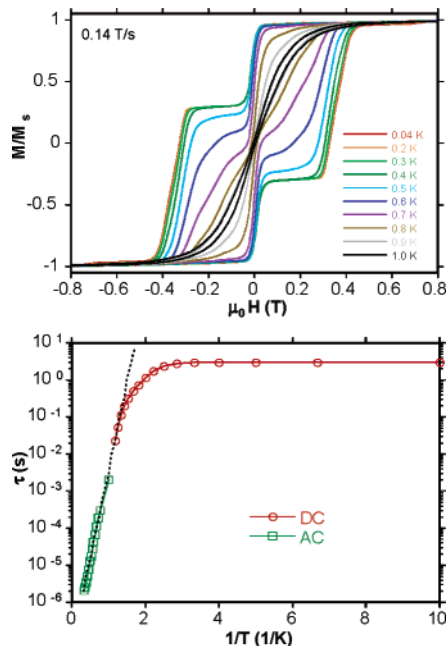


**Figure 4.** (Top) Magnetization versus field hysteresis loops for a single crystal of  $2 \cdot 3\text{CH}_2\text{Cl}_2$  at the indicated temperatures;  $M$  is normalized to its saturation value,  $M_S$ . (Bottom) Arrhenius plot constructed from AC  $\chi_M''$  versus  $T$  and DC magnetization decay versus time data. The dashed line is the fit of the thermally activated region to the Arrhenius equation.

Since **2** has significant  $S$  and  $D$  values, we investigated whether it is a SMM by AC susceptibility measurements in a 3.5 G AC field (Figure 3). Indeed, a frequency-dependent decrease in the in-phase ( $\chi_M'$ ) signal<sup>9</sup> and a concomitant out-of-phase ( $\chi_M''$ ) signal were seen at  $<3$  K (Figure 3), indicative of the slow magnetization relaxation of SMMs. Since intermolecular interactions and phonon bottlenecks can also give such signals,<sup>12</sup> confirmation that **2** is a SMM was sought by magnetization versus DC field scans on single crystals of  $2 \cdot 3\text{CH}_2\text{Cl}_2$  using a micro-SQUID.<sup>13</sup> Hysteresis, the diagnostic property of a magnet, was observed below  $\sim 1.0$  K (Figure 4, top). The loops exhibit increasing coercivity with decreasing temperature and increasing field sweep rate,<sup>9</sup> as expected for a SMM. The loops also display the steps indicative of QTM between  $M_S$  levels of the  $S = 6$  ground state, with the temperature independent coercivity at  $\leq 0.3$  K, indicating ground state QTM, that is, only between the lowest energy  $M_S = \pm 6$  levels.

AC data to lower  $T$  and magnetization decay versus time data were collected and used to construct Figure 4 (bottom), based on the Arrhenius relationship  $\tau = \tau_0 \exp(U_{\text{eff}}/kT)$ , where  $U_{\text{eff}}$  is the effective relaxation barrier,  $\tau$  is the relaxation time, and  $k$  is the Boltzmann constant. The slope in the thermally activated region gave  $U_{\text{eff}} = 10.9$  K and  $\tau_0 = 5.7 \times 10^{-8}$  s. Below 0.3 K, the

relaxation was temperature-independent, consistent with relaxation by ground-state QTM.

Complex **2** is thus confirmed to be a SMM, the first with a triangular topology. What now demands explanation is why **2** is ferromagnetically coupled and a SMM whereas the many previous triangular  $[\text{Mn}_3\text{O}(\text{O}_2\text{CR})_6\text{L}_3]^+$  complexes (such as **1**) are antiferromagnetically coupled and are not? We believe the answer is that **2** has its central  $\text{O}^{2-}$  ion  $0.295 \text{ \AA}$  above the  $\text{Mn}_3$  plane due to the tridentate binding of the  $\text{mpko}^-$  ligand, whereas the  $\text{O}^{2-}$  ion in **1** and related species is in the  $\text{Mn}_3$  plane, or essentially so ( $<0.03 \text{ \AA}$ ). The central  $\text{O}^{2-}$  strongly mediates antiferromagnetic exchange via  $M_{\text{d}\pi}-\text{O}_{\text{prt}}-M_{\text{d}\pi}$  orbital overlap, and any distortion away from planarity will thus weaken antiferromagnetic contributions to the observed exchange,  $J_{\text{obs}}$ , between two Mn atoms. Since  $J_{\text{obs}}$  is the sum of ferro- and antiferromagnetic contributions, and  $J_{\text{obs}}$  is in any case only weakly antiferromagnetic in  $[\text{Mn}_3\text{O}(\text{O}_2\text{CR})_6\text{L}_3]^+$  complexes,<sup>5</sup> it is reasonable that structural distortion to a nonplanar  $[\text{Mn}_3\text{O}]^{7+}$  core would lead to ferromagnetic  $J_{\text{obs}}$  and a resultant  $S = 6$  ground state.<sup>14</sup>

In conclusion, the distortion imposed on a  $[\text{Mn}_3\text{O}]^{7+}$  member of the venerable class of triangular, oxide-centered  $[\text{M}_3\text{O}]^{6+,7+}$  complexes by a tridentate oximate ligand switches the exchange coupling to ferromagnetic and makes **2** the initial example of a triangular SMM. This suggests that it may also be possible to modify other triangular (or other) structures with chelating and/or bridging ligands to switch on the properties of a SMM.

**Acknowledgment.** Th.C.S. and S.P.P. thank the Program PYTHAGORAS (Grant b.365.037) for funding. G.C. thanks the U.S.A. National Science Foundation (Grant CHE-0414155).

**Supporting Information Available:** Crystallographic details in CIF format, bond valence sums, and magnetism data. This material is available free of charge via the Internet at <http://pubs.acs.org>.

## References

- (1) Christou, G.; Gatteschi, D.; Hendrickson, D. N.; Sessoli, R. *MRS Bull.* **2000**, *25*, 66–71 and references therein.
- (2) (a) Sessoli, R.; Gatteschi, D.; Caneschi, A.; Novak, M. A. *Nature* **1993**, *365*, 141–143. (b) Sessoli, R.; Tsai, H. L.; Schake, A. R.; Wang, S.; Vincent, J. B.; Folting, K.; Gatteschi, D.; Christou, G.; Hendrickson, D. N. *J. Am. Chem. Soc.* **1993**, *115*, 1804–1816.
- (3) Friedman, J. R.; Sarachik, M. P.; Tejada, J.; Ziolo, R. *Phys. Rev. Lett.* **1996**, *76*, 3830.
- (4) Wernsdorfer, W.; Sessoli, R. *Science* **1999**, *284*, 133–135.
- (5) (a) Vincent, J. B.; Chang, H.-R.; Folting, K.; Huffman, J. C.; Christou, G.; Hendrickson, D. N. *J. Am. Chem. Soc.* **1987**, *109*, 5703–5711 and references therein. (b) Jones, L. F.; Rajaraman, G.; Brockman, J.; Murugesu, M.; Sanudo, C. E.; Raftery, J.; Teat, S. J.; Wernsdorfer, W.; Christou, G.; Brechin, E. K.; Collison, D. *Chem.—Eur. J.* **2004**, *10*, 5180.
- (6) For a review, see: Miliou, C. J.; Stamatatos, Th. C.; Perlepes, S. P. *Polyhedron*, in press, and references therein. (b) Weyhermueller, T.; Wagner, R.; Khanra, S.; Chaudhuri, P. *Dalton Trans.* **2005**, 2539.
- (7) Anal. Calcd (found) for dried **2** (solvent-free): C 37.59 (37.32), H 3.50 (3.49), N 9.74 (9.54). Crystal data for  $2 \cdot 3\text{CH}_2\text{Cl}_2$ :  $\text{C}_{33}\text{H}_{36}\text{N}_6\text{O}_{14}\text{Cl}_7\text{Mn}_3$ , 1117.54 g mol<sup>-1</sup>, monoclinic  $P2_1/c$ ,  $a = 12.986(5) \text{ \AA}$ ,  $b = 14.978(6) \text{ \AA}$ ,  $c = 23.150(10) \text{ \AA}$ ,  $\beta = 93.82(2)^\circ$ ,  $Z = 4$ ,  $V = 4493(3) \text{ \AA}^3$ ,  $d_{\text{calcd}} = 1.492 \text{ g cm}^{-3}$ ,  $T = 293(2) \text{ K}$ . Final  $R1 = 6.96$  and  $wR2 = 19.36\%$ .
- (8) (a) Liu, W.; Thorp, H. H. *Inorg. Chem.* **1993**, *32*, 4102–4105. (b) BVS for the  $\text{Mn}^{3+}$  and  $\text{O}^{2-}$  ions were 3.03–3.12 and 2.08, respectively.
- (9) See Supporting Information.
- (10) The fit gave  $J = +14.1 \text{ cm}^{-1}$ ,  $J' = +3.8 \text{ cm}^{-1}$ ,  $g = 1.91$ , and 0.9% paramagnetic impurity term; the TIP was held constant at  $600 \times 10^{-6} \text{ cm}^3 \text{ mol}^{-1}$ . Equilateral  $[\text{M}_3\text{O}]$  triangles undergo the magnetic Jahn–Teller distortion, resulting in an isosceles ( $2J$ ) situation. See: Cannon, R. D.; Jayasooriya, U. A.; Wu, R.; arapKoske, S. K.; Stride, J. A.; Nielsen, O. F.; White, R. P.; Kearley, G. J.; Summerfields, D. *J. Am. Chem. Soc.* **1994**, *116*, 11869–11874 and references therein.
- (11) The fit for the propionate analogue of **2** gave  $S = 6$ ,  $g = 1.93$ , and  $D = -0.34 \text{ cm}^{-1}$ ; this complex gives the same ac susceptibility data as **2**.
- (12) Chakov, N. E.; Wernsdorfer, W.; Abboud, K. A.; Christou, G. *Inorg. Chem.* **2004**, *43*, 5919–5930.
- (13) Wernsdorfer, W. *Adv. Chem. Phys.* **2001**, *118*, 99–190.
- (14) The  $D$  value will also be affected by this distortion, as the single-ion anisotropy axes are tilted. Details will be provided in the full paper.

JA0558138